Bulletin of the Seismological Society of America, Vol. 96, No. 2, pp. 624–636, April 2006, doi: 10.1785/0120050114

Seismicity and State of Stress in the La Paz–Los Cabos Region, Baja California Sur, Mexico

by Luis Munguía, Mario González, Sergio Mayer, and Alfredo Aguirre

Abstract We present the results of an analysis of seismic data collected for seven years in the La Paz–Los Cabos region. The data set includes earthquakes with magnitudes of up to 3.6 and focal depths mostly between 2 and 14 km. The results show that some located epicenters correlated with known faults of the region, but others did not, suggesting faults that have not yet been recognized. In addition, even though earthquakes occurred all over the study area, zones of stress concentration were identified. In such zones, the seismicity often developed as earthquake swarms. Composite fault-plane solutions were prepared by using data of those areas. The resulting mechanisms for events of the northern part of the study area indicated normal faulting (east-side down). In such case, the *P* axis had a mean vertical angle of 55° in the N12° W direction, whereas the *T* axis was nearly horizontal and with a N68° E average trend. This part of the study area is found to be under a predominant tensional stress regime. To the southwest of the area, the focal mechanisms showed predominant components of strike-slip faulting. There, the *T* axes were still subhorizontal, but the *P* axes were more horizontal, resulting in a mean plunge of about 20° in the N38° W direction.

On the other hand, highly consistent directions of *P* and *T* axes from 13 representative events of the Gulf of California fault system led to average axes that are close approximations to the principal stresses that drive such a fault system. A comparison of these axes with average *P* and *T* axes of our region shows that the latter are about 16 to 23 degrees more westerly than the former. We propose then either that the earthquakes in the study area occur more in response to local tectonic forces, or that our inferred stress axes are only approximations to the principal stresses. The complex tectonic situation of the region makes the first possibility feasible, but the fact that the earthquakes occurred on pre-existing faults favors the second one. Future seismic data of the region will help to elucidate this uncertainty.

Finally, the microearthquakes studied were not generated by the Gulf of California fault system that forms the boundary between the Pacific and North America plates. Our results, then, are evidence of a wide zone of deformation across which subsidiary faulting accommodates part of the relative plates motion.

Introduction

The La Paz–Los Cabos region is located to the west of the boundary between the Pacific and North American plates, a boundary that extends throughout the Gulf of California. Located between 22.5–25.0° north latitude and 109.0–111.0° west longitude, the study region comprises the southernmost part of the Baja California peninsula (Fig. 1). According to Worldwide Earthquake Catalogs of the Advanced National Seismic System (ANSS), this region was relatively quiet before 30 June 1995, when earthquakes of *M* 6.2 and 5.4 occurred north of the city of La Paz (Fletcher and Munguía, 2000). Prior to those events, only two relevant earthquakes of *M* 5.6 and 5.0 had occurred on 4 and 18 April 1969 east of Cerralvo island, and two *M* 5.3 events on 21 and 22 August 1969 in the Pacific Ocean, southwest of Todos Santos (Molnar, 1973; Goff *et al.*, 1987).

The occurrence of the June 1995 strong events evidenced the reactivation of a fault located along the eastern flank of the Espíritu Santo and La Partida islands. Before those earthquakes, little was known about the seismicity of the area, in part, because of the nonexistence of seismic stations in the region. In the first microearthquake study of the region, Munguía *et al.* (1992) reported the occurrence of

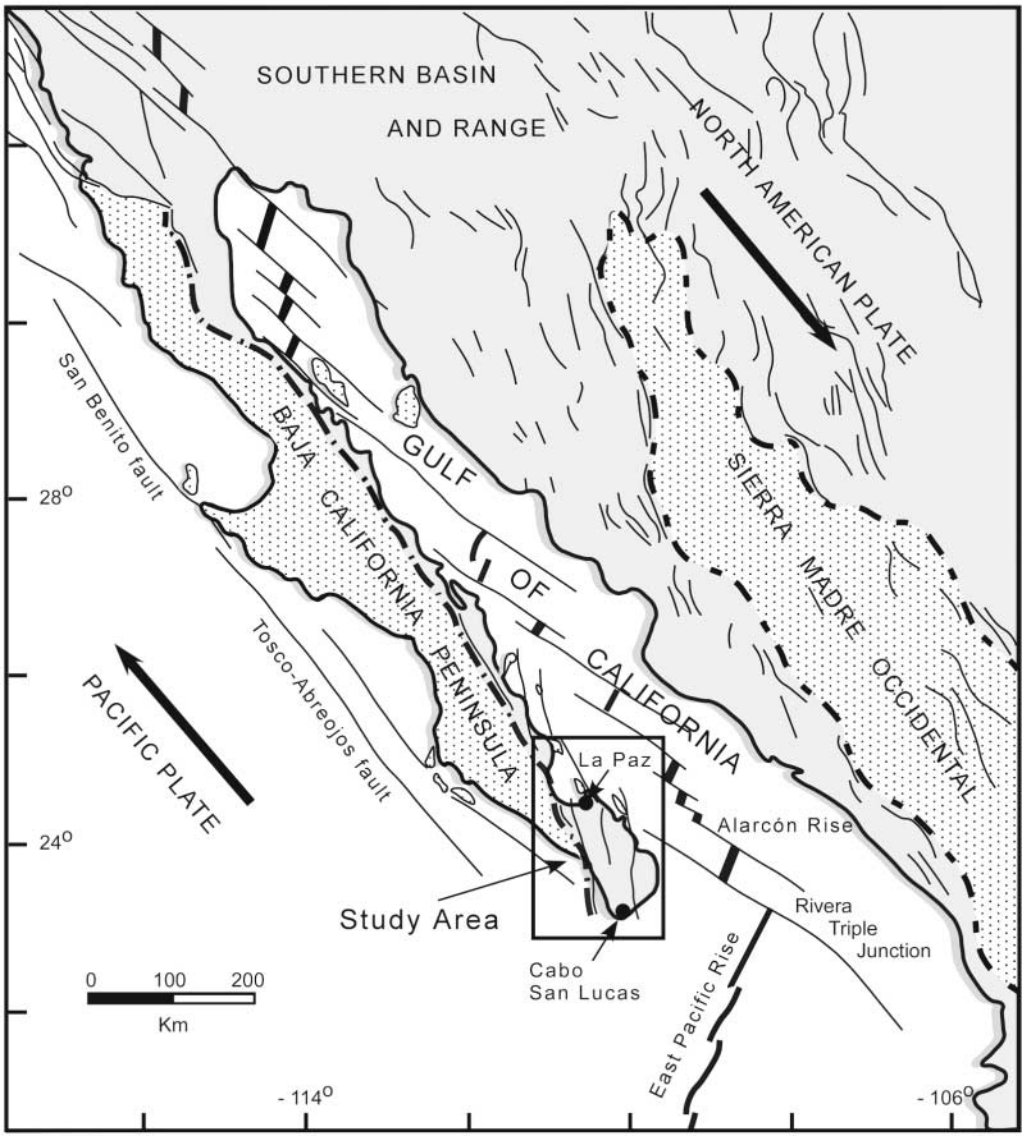

Figure 1. Map showing the dominant quaternary fault systems (thin lines) in the Gulf Extensional Province and the Southern Basin and Range Province. The main boundary between the Pacific and North America plates is formed by a series of nascent ocean-spreading centers (heavy line segments) that are connected with transform faults (thin lines) along the Gulf of California. This system connects the East Pacific rise at the south with the San Andreas Fault system to the north (SAF in the figure). Heavy dash-dotted lines represent terrain boundaries. The area of the present study is indicated with a rectangle. (Modified from Fletcher and Munguía, 2000).

about 150 microearthquakes with magnitudes of up to 2.7. About one third of those events were recorded during July and August 1989 in a two-day swarm that occurred near the aftershock zone of the 30 June 1995 earthquakes. The rest of the seismicity occurred during the entire 40-day period of recording, with epicenters scattered east of the city of La Paz.

In a more recent study, Fletcher and Munguía (2000) analyzed the data set recorded for aftershocks of the 1995 La Paz earthquakes. This data set was analyzed together with geologic information and data of some historical events of the region. Results of the study indicate that a fraction of the Pacific-North American plate motion is being accommodated by sets of normal and strike-slip faults located to the west of the boundary between the plates. They suggested that continental rifting and seafloor spreading in the region have occurred simultaneously during the past 3.6 Ma. Nevertheless, the necessity of a more detailed study for a better understanding of the pattern and kinematical evolution of faulting in the La Paz–Los Cabos region was clear at that time.

A study of seismicity in the La Paz–Los Cabos region

is important for two main reasons. First, earthquakes of intermediate magnitude have occurred in the region, a fact of importance from the point of view of the seismic risk for about 200,000 inhabitants of La Paz City and other less populated areas in the region. Second, a more complete understanding of the seismotectonic structure of the region could be useful as a constraint in global models of the relative motion of the Pacific and North American plates.

In this article, we present results of a first attempt in monitoring the microseismic activity of the entire La Paz–Los Cabos region. Such results include a description of the main characteristics of the recorded seismicity and a discussion of the stress pattern that was inferred from composite fault-plane solutions.

Tectonic Frame

Tectonically, the La Paz–Los Cabos region forms part of the Gulf Extensional Province (Fig. 1). The most important geomorphic feature in the region is a prominent crystalline block, known as Los Cabos block, which rises to heights that can be of up to 2000 m. The Mesozoic batholithic rocks that constitute this block are clearly distinguishable from the volcanogenic strata that characterize most of the study region (Aranda-Gómez and Pérez-Venzor, 1997; Fletcher and Munguía, 2000; Bravo-Pérez, 2002, and references therein).

Flanked by the Gulf of California to the east and the Pacific Ocean to the west, the La Paz–Los Cabos region is crisscrossed by several major active faults, like the Espíritu Santo, San José del Cabo, El Carrizal, San Bartolo, and San Juan de Los Planes faults (Fig. 2). These features trend approximately north-northwest and control the position and geometry of three major Quaternary basins in the area. Except for the San Bartolo fault that dips west, the other faults are east-down normal faults that accomplish east-northeast extension, as evidenced by fault segments that cut Quaternary alluvial fan deposits in the region (Fletcher and Munguía, 2000). These faults dominate the mode of faulting and are responsible for the westward tilting of the Miocene volcanic rocks and asymmetric uplift of the Los Cabos Block (Fletcher *et al.*, 2000). In addition, the La Paz–Los Cabos region is also cut by a set of near-parallel, west-northwest-striking, left-lateral faults that are best exposed in the southern portion of the Los Cabos crystalline block (Bravo-Pérez, 2002). As seen in Figure 2, these faults have lengths ranging from 8 to 23 km and are separated by ~ 5–8 km.

Historically, before ~29 Ma the Farallon and other microplates were subducting along the western margin of the American continent (Atwater, 1970, 1989). About 12 m.y.a., when the western North America subduction process ceased and the plate-margin slip concentrated mostly in the Gulf of California, the Pacific plate began the capture of the Baja California microplate (Atwater, 1989; Bohannon and Parsons, 1995). At that time, the Rivera triple junction began migrating southeast, toward its present location.

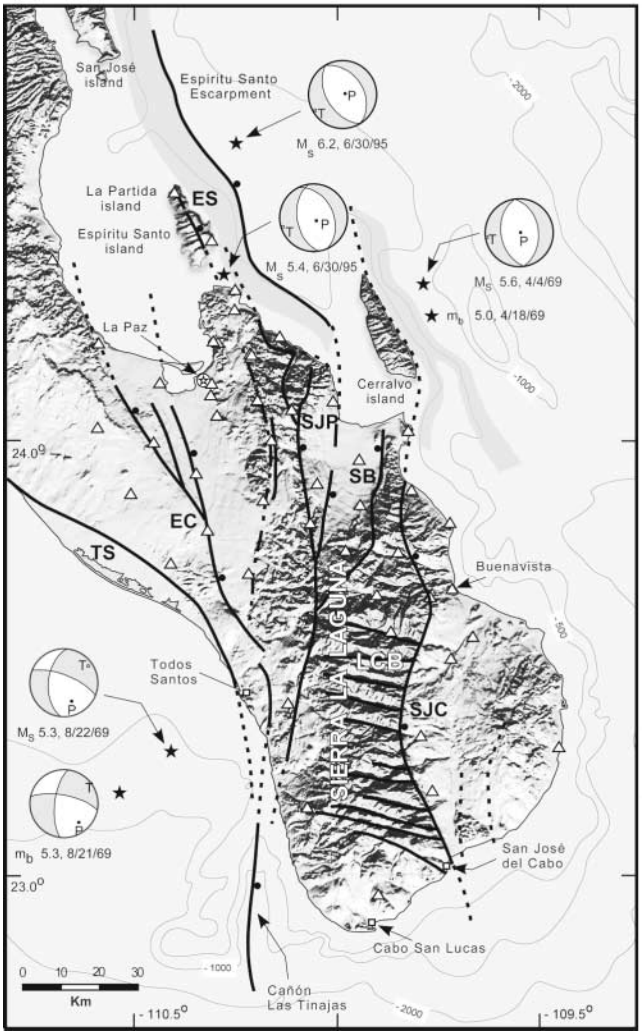

Figure 2. Map of the La Paz–Los Cabos region showing recognized and inferred faults (heavy and dash lines, respectively), historical earthquakes (stars), and sites of seismic stations (triangles). Black dots are drawn on the hanging wall of normal faults. The west-northwest-striking faults that cut Los Cabos Block are strike-slip sinistral faults predominantly. The beach balls represent the focal mechanisms for some past earthquakes. Gray-shaded strips, located east of the Cerralvo and Espíritu Santo islands, indicate major east-facing bathymetric escarpments. Abbreviations: EC, El Carrizal fault; SJP, San Juan de Los Planes fault; ES, Espíritu Santo fault; SB, San Bartolo fault; SJC, San José del Cabo fault; TS, Todos Santos fault; LCB, Los Cabos Block.

To date, most of the relative motion between the Pacific and North American plates takes place along the transform fault systems in the Gulf and Salton trough (e.g., DeMets, 1995). However, as Humphreys and Weldon (1991) pointed out, the spreading rate that is observed across the Alarcón rise, near the mouth of the Gulf of California, is less than the 56–60 cm total rate of slip obtained in global plate-motion studies. Thus, it is thought that some plate motion is

being accommodated on faults of the coastal and offshore zones west of the main plate boundary in Baja California and California (e.g., Minster and Jordan, 1987; Weldon and Humphreys, 1986).

In a kinematic model for the Pacific-North America plate motion, Dixon *et al.* (2000) showed evidence that all or part of the Baja California peninsula (south of the Agua Blanca fault) is not completely transferred to the Pacific plate. In their study, Fletcher and Munguía (2000) analyzed seismic data from sets of active faults in the La Paz–Los Cabos region. Based on the earthquake characteristics of those fault systems, they also proposed that this portion of the Baja California peninsula might not be rigidly coupled to the Pacific plate. Thus, the assumption that the Baja California peninsula was transferred completely to the Pacific plate by 3.6 m.y.a. when seafloor spreading commenced along the Gulf rise in the southern Gulf of California might not be valid (DeMets, 1995). Detailed reviews of the tectonics and fault systems of the La Paz–Los Cabos region can be found in articles by Normark *et al.* (1987), Fletcher and Munguía (2000), and Bravo-Pérez (2002), among several others.

Data Collection

The seismic data set was recorded with ten digital three-component accelerographs and six analog (smoked-paper) seismographs. Six digital stations were equipped with Kinemetrics Altus K2 recorders and EpiSensor accelerometers (FBA ES-T). The other four consisted in K2 accelerographs with internal force-balanced sensors (FBA-23). Because of the character of our study, the digital instruments were set to record ground acceleration amplitudes of up to $0.5g$ (g = 981 cm/sec^2) at a rate of 200 samples per second. The analog stations consisted of Kinemetrics seismometers (Ranger SS-1) of 1-sec natural period coupled to Sprengnether seismographs (MEQ-800B). Such stations recorded only the vertical component of motion at gain settings of 66–84 dB, depending on the signal-to-noise ratio at each site. The station coordinates were determined with Global Positioning Systems (GPS).

At the initial stage of the project, only five analog stations were operated in the northern part of the study area. With this sparse network, we recorded the seismicity that occurred in the neighborhood of La Paz from September 1996 to December 1997. Despite that the fieldwork was performed in an irregular temporal basis, a continuous microseismic activity was always observed in the aftershock zone of the June 1995 La Paz earthquakes.

The purpose of the present study was to monitor the microseismic activity of the entire La Paz–Los Cabos region, that is, from La Partida–Espíritu Santo islands to Cabo San Lucas (Fig. 2). With this goal, by October 1998, we began the installation of ten digital accelerographs and six analog seismographs in the northern part of the study area. After some time of operation with the first configuration of the network, most of the stations were removed and reinstalled in a new area. This process of removal/reinstallation of stations was repeated in such a way that in the five-year period of recording the network was installed in six different areas. Each time the network recorded from 5 months to more than one year, depending on the seismic activity of each area.

The triangles in Figure 2 mark all 36 sites that were occupied with seismic instrumentation for 7 years. During this period, many acceleration signals were recorded for microearthquakes with moment magnitudes of up to 3.6. However, since most of the digital data correspond to events of small magnitudes, the peak amplitudes on the waveforms are of the order of a few cm/sec^2. Exceptions to that were the signals recorded within 6 km from the sources for an earthquake series occurred in August 2002 in association with the San José del Cabo fault (zone D in Fig. 3). In this case, a peak ground acceleration of 150 cm/sec^2 was recorded at 3 km from the epicenter of the largest earthquake of the series (M_w 3.5). Because most of the recorded ground accelerations were small, a detailed analysis of such acceleration data was not considered for this study. We only took advantage of the high-quality digital recordings to make accurate readings of the *P*- and *S*-wave arrival times for the hypocenter location process.

Data Analysis and Results

Hypocenter Locations

The seismic data were analyzed by using version 7.2 of the SEISAN software package (Havskov and Ottemöller, 2001). The crustal velocity model of Fletcher and Munguía (2000) was used in the hypocenter location process. This model consists of four layers over a half-space with the following *P*-wave and thickness characteristics, respectively: 4.0 km/sec, 2 km; 6.0 km/sec, 5 km; 6.4 km/sec, 7 km; and 6.9 km/sec, 10 km. The lower infinite half-space has a *P*-wave velocity of 7.6 km/sec. Wadati diagrams prepared with the arrival times led us to an average V_P/V_S ratio of 1.73 for the entire La Paz–Los Cabos region. With this V_P/V_S value, the *S*-wave velocity was calculated and used in the hypocenter location process. The location computer code of Lienert and Havskov (1995) was used to determine the hypocenter locations.

About 40% of the recorded events were located with errors of less than 3 km in both epicenter and focal depth. This rather low proportion of better-located events results from two facts. First, at the beginning of the project the seismicity of the region was monitored with only five analog stations. The azimuthal coverage provided by such a small array was poor. Second, each temporary network installed from October 1998 to December 2003 had more stations, but because of the small size of the earthquakes to be recorded, the covered areas were smaller too. Thus, the location errors for events occurring outside a given network were larger than for events occurring inside the network. Despite

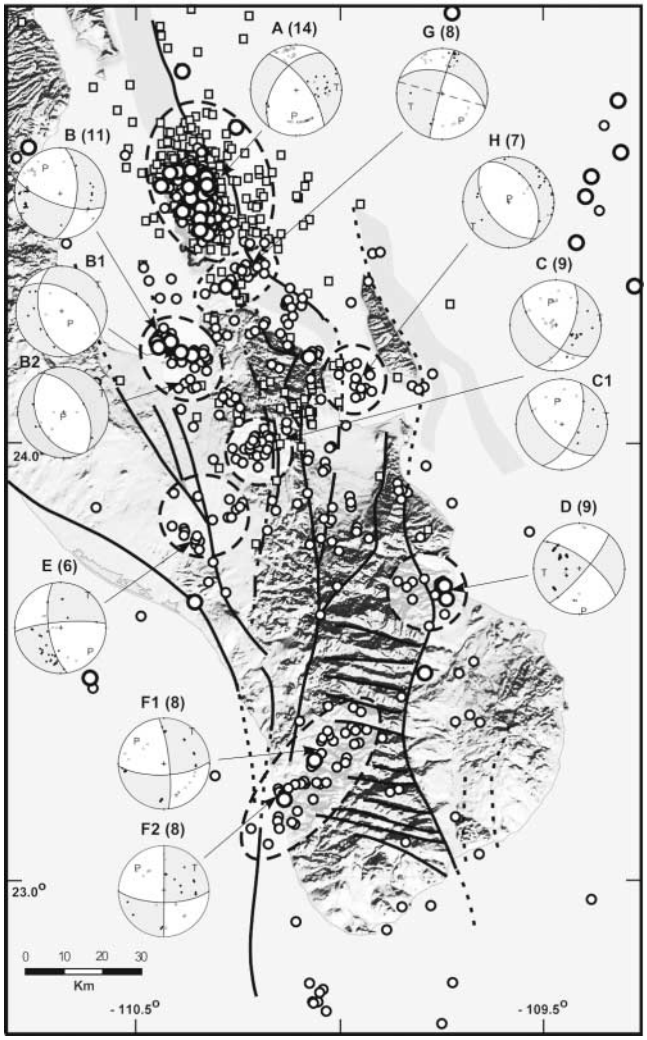

Figure 3. Epicenter distribution of earthquakes analyzed in this study. Squares represent seismicity of the 1996–1997 period, and circles indicate events of the 1998–2003 period. The larger circles represent events with magnitudes greater than or equal to 3.0 from both periods. The beach balls correspond to individual and composite fa plane solutions for earthquakes that occurred in the areas enclosed by discontinuous lines. Capital letters above the focal mechanisms identify the zones of activity; the figures in parentheses indicate the number of events that provided data for the fault-plane solution. Single-event fault-plane solutions are labeled as B1, B2, and C1. See Figure 2 for legend and geologic features.

this, it was found that the main characteristics of the epicenter distribution are kept when only the higher quality epicenters are considered.

Magnitude Calculations

An important issue in seismic data analyses is the calculation of magnitudes for the earthquakes under study. Here, three types of magnitude were determined, namely, M_c, M_L, and M_w. The coda magnitude, M_c, was calculated from the signal durations that were measured on analog records. Thus, this type of magnitude was assigned to earthquakes that were recorded at the beginning of the project, when only analog stations were in operation. Due to the lack of a magnitude-distance relationship for the La Paz–Los Cabos region, the coda magnitudes were calculated by using the empirical relationship of Lee *et al.* (1972). This relationship is based on data from earthquakes that occurred in California, so we used it with the initial purpose of getting an approximate estimate of the size of the recorded events.

The local magnitude, M_L, on the other side, was calculated through a standard technique proposed by Kanamori and Jennings (1978). This technique uses Richter's (1958) definition of local magnitude with zero-to-peak amplitudes from synthetic Wood-Anderson records. To apply this approach on data from the La Paz–Los Cabos region, a $-\log A_0$ attenuation function proper for the region was determined in a separate analysis of the digital data (González *et al.*, unpublished manuscript, 2005). With such attenuation function, reliable local magnitudes were assigned to the microearthquakes evaluated in this study.

The third type of magnitude calculated, M_w, was obtained from the seismic moment, M_0, of the earthquakes (Ottemöller and Havskov, 2003). In this case, the seismic moment was obtained first via standard spectral analysis of the *S*-wave horizontal signals. Then, the moment was converted to magnitude in the way suggested by Kanamori (1977). Given that M_0 is calculated directly from the spectra of *S*-wave signals, the moment magnitude is considered more precise than the other two magnitudes. On the other hand, it has been widely observed that for earthquakes smaller than $M_w \sim 4.0$, the moment magnitude compares well with the M_c or M_L magnitudes. In the past five years, our temporary networks operated with analog and digital stations. This fact allowed us to verify that the three magnitude scales have comparable results. From a set of nearly 300 microearthquakes, 85% of the calculated magnitudes differed in the worst cases by no more than ± 0.4 units. In all three scales of magnitude, the calculated magnitudes for earthquakes of the whole database are between 1.0 and 3.6.

Distribution of Epicenters

The spatial distribution of the 1030 earthquakes for which epicenters were determined is shown in Figure 3. Squares and circles in the figure represent earthquakes recorded in the 1996–1997 and 1998–2003 periods, respectively. The larger-size circles indicate epicenters for about 40 events that had magnitudes between 3.0 and 3.6. As seen on the figure, the La Paz–Los Cabos region has been relatively active over the past 7 years. Despite the observation that the located microseismicity is scattered all over the study area, clear epicenter trends and clusters are well defined. Such features thus reveal zones in which stresses accumulate and release more often in the region. These areas,

denoted with the letters A to H in Figure 3, have been delimited with closed discontinuous lines. The seismicity in those areas often develops as swarms of earthquakes of varying intensity and temporal duration. On the other hand, note that some epicenters may be correlated with some of the mapped faults of the region. Examples of this are the epicenters located along the northern segment of the San José de Los Cabos fault, along a north strand and the central segment of the El Carrizal fault, and most notoriously along the eastern flank of the Espíritu Santo and La Partida islands. To the south of these islands the seismicity is more diffuse, though some of it may be associated to strands of the San Juan de Los Planes fault. The epicenters that do not correlate with any recognized fault of the region constitute evidence of structural features that have not yet been recognized geologically. The seismicity that is denoted as zone F in the Figure 3 is a clear example of this.

Fault-Plane Solutions

Because of the low magnitude of the recorded events and our limited number of seismic stations, single-event fault-plane solutions were difficult to obtain in the present study. Only three events were the exception to this. For each one of these events the number of recording stations was enough to obtain a single-event fault-plane solution. Thus, because of data shortage, most of the focal mechanisms included in this article correspond to composite fault-plane solutions.

To get the individual and composite fault-plane solutions we used FOCMEC (Snoke *et al.*, 1984), a program that forms part of the SEISAN computer package. In all cases, the mechanisms are equal-area, lower-hemisphere plots of *P*-wave first-motion data from groups of events with magnitudes between 1.5 and 3.6. To get the composite mechanisms, we used *P*-wave polarity data from 6 to 14 closely spaced events. In this process, we included well-located events with hypocenters falling in zones of less than 2-km radius in both horizontal and vertical directions. Some of these events occurred closely spaced in time, but others did not. For instance, 10 of the 11 events that were used to obtain the composite fault-plane solution for zone B occurred in November 1998. In addition, the mechanisms for the zones D and G were determined with the data from events that occurred in 3-day and one-month periods, respectively. Fault-plane solutions for the other zones are based on data from events that occurred more separated in time but still recorded with the same network configuration. Despite this, the consistency observed among the *P*-wave first motions is good, and thus we have implicitly assumed that all the events in the clusters were generated by the same style of faulting. All the focal mechanisms that were determined for the chosen areas of activity are shown in the map of Figure 3. The parameters related to those fault-plane solutions are summarized in Table 1, and brief descriptions of the mechanisms are given in the next section.

Interpretations of Earthquake Faulting

First, our study comprises a large proportion of the located epicenters felt in the area of the Espíritu Santo and La Partida islands (zone A in Fig. 3). As indicated earlier, those events are the result of motion along the Espíritu Santo fault, a fault that generated the 30 June 1995 moderate earthquakes (Fletcher and Munguía, 2000). The intense aftershock activity that followed those events lasted for four and a half years, ceasing by the end of 1999. For most of the better-located events of this particular area, the focal depths calculated ranged from 1 to 12 km. The M_L and M_w magnitudes calculated for earthquakes of this zone reached values of up to 3.4.

Figure 4 shows a closeup of the Espíritu Santo and La Partida islands area, along with epicenters of well-located events. This figure includes a composite fault-plane solution and a plot of focal depth projected onto a southwest–northeast-oriented vertical plane. First-motion data of 14 events were used in the preparation of the fault-plane solution. The focal depths of the events used are between 4.0 and 7.0 km, whereas the epicenters are within a circular zone of less than a 3-km radius. Although considerable scatter is seen in the projected focal depth, the data slightly suggest that the earthquake sources deepen to northeast. Such an observation is consistent with the fault plane that dips N50° E in the composite fault-plane solution.

In the La Paz Bay area (zone B), the seismicity developed mainly in the form of earthquake swarms. One of the more intense swarms of the area began on 20 October 1998. Although earthquakes in this swarm occurred for the next 10 months, the greatest number of events was observed during the first two months of activity. Thirty-two events of this area were located near the inferred north strand of the El Carrizal fault (see Fig. 2) at focal depths that range from 4.0 to 12.0 km. The residents of La Paz city felt the effects of the largest earthquake in this swarm (M_w 3.6), which occurred on 22 November 1998 at 18 km north of the city.

Figure 5 shows a map of epicenters, a vertical focal depth profile, and fault-plane solutions for earthquakes of the La Paz Bay area. The first fault-plane solution on the right of the figure is based on data of 11 earthquakes with source depths between 5 and 7 km. The epicenters of those events lie closely spaced within the rectangular area that is shown in Figure 5. Note that the nodal plane that dips east in the focal mechanism is in agreement with the AB vertical cross section that is included in the figure. Then, both focal mechanism and focal depth profile indicate that the clustered events deepen in an east-northeast direction. Note also that, given the location of these closely spaced events, it is likely that they occurred in association with the north strand of El Carrizal fault (CFNS) that is shown in Figures 2 and 5. The almost eastwest focal depth profile for this zone was chosen nearly perpendicular to this fault strand. However, other source-depth profiles with a more southwest–northeast orientation defined slightly better the trend of earthquake

Table 1
Parameters Related to the Composite and Individual Fault-Plane Solutions for Earthquakes of the La Paz–Los Cabos Region

	Plane 1		Plane 2		*P* Axis		*T* Axis		No. of
Zone	Strike	Dip	Strike	Dip	Azimuth	Plunge	Azimuth	Plunge	Events
A	215	50 NW	323	70 NE	185	45	84	12	14
B	6	60 ESE	108	70 SSW	330	36	240	2	11
B1	166	50 WSW	302	50 NE	144	65	54	0	1
B2	158	40 SW	328	50 NE	191	83	62	6	1
C	24	60 ESE	135	60 SW	348	45	78	2	9
C	24	60 ESE	135	60 SW	348	45	78	2	1
D	308	70 NE	40	80 SE	176	10	264	20	9
E	172	70 WSW	266	80 NNW	130	20	40	6	6
F1	356	80 E	88	70 S	310	22	40	4	8
F2	0	90	90	70 S	312	14	46	14	8
G	194	84 WNW	288	50 NNE	144	30	250	24	8
H	334	40 NE	143	50 SW	8	82	237	5	7

The letters in the first column indicate the zones of the focal mechanisms. All angles in this table are in units of degrees. Azimuth and strike angles are measured clockwise from the north. The last column of the table gives the number of earthquakes used for each fault-plane solution.

source deepening. In such instances, the angle that the dashed line makes with the horizontal was slightly lower. This observation suggests that either the El Carrizal fault strand is more westerly oriented than it was drawn in Figures 2 and 5, or that the earthquakes were generated on a still unrecognized northwest-striking normal fault. The second possibility, however, would be inconsistent with the fault-plane solution that was determined for that group of events. Future seismic data collected in this area will help to elucidate such uncertainty.

The mechanisms B1 and B2 of Figure 5, on the other hand, are individual fault-plane solutions for two earthquakes located just southeast of the main concentration of events. Those earthquakes differ from the group of events used in the determination of the previous composite focal mechanism in two ways. First, the earthquakes occurred deeper in the crust, at 10- and 12-km depths, and second, their mechanisms show almost pure normal faulting. In addition, these events have epicenters that do not correlate with the northerly inferred strand of the El Carrizal fault or with any other known fault in the area. Rather, they appear to be more representative of northwest-striking normal faults in the area. Based on the north-northeast direction of earthquake source deepening observed for the zone, the nodal planes that dip northeast in the mechanisms might be suggested as the planes of fault motion for these earthquakes.

The seismicity located just south-southeast of zone B, as well as that of zone C, and the events that lie in between this zone and zone H occurred deeper in the crust. In such cases, the determined source depths range between 8 and 15 km. To the east of those events, in particular in zones G and H and the cluster of events located between zones C and H, the earthquakes occurred at shallower source depths. In those places, the focal depth varied from 1 to 8 km.

Another seismicity trend of interest has been marked as zone F in the Figure 3. In this zone, the data gathering was performed with stations installed on the southern part of the study area during 2002 and 2003. Most of the earthquake sources that were located there have depths that go from 2 to about 13 km. The epicenters define an elongated zone of about 40 km long and 15 km wide, with its major axis trending in a N45° E direction. However, as Figures 2 and 3 show, none of the mapped faults of the area has this orientation, which made us think of two possibilities. One, the seismicity is produced by a still unrecognized northeast-striking fault in the area. Two, the events are the result of motion along west-northwest-striking faults that have been mapped in the southern portion of the Los Cabos crystalline block. Though the observed northeast epicenter alignment supports the first possibility, the fault-plane solutions for these events (discussed next) agree with the second one. More seismic and geologic data are needed to reach a definite answer regarding the kinematics of faulting in this zone.

Figure 6 shows the composite fault-plane solutions that were obtained for two groups of eight events each in zone F. The epicenters of events in each group are located around center points that are separated by no more than 10 km from each other; In addition, the focal depths for most events in these groups are between 5 and 7 km. Figure 6 shows that the fault-plane solutions are consistent among themselves, even though they were obtained separately for each group. Molnar (1973) reported focal mechanisms for two *M* 5.3 earthquakes that occurred in the Pacific Ocean, at 35–45 km to the west of zone F (see Fig. 6). A comparison of Molnar's mechanisms with the focal mechanisms of this study shows consistency among the strike angles of fault planes in both sets of mechanisms. Even though the dip angles of fault planes in those mechanisms are not well constrained by data, the last observation suggests that in this part of the study area the mode of faulting is primarily of the strike-slip type.

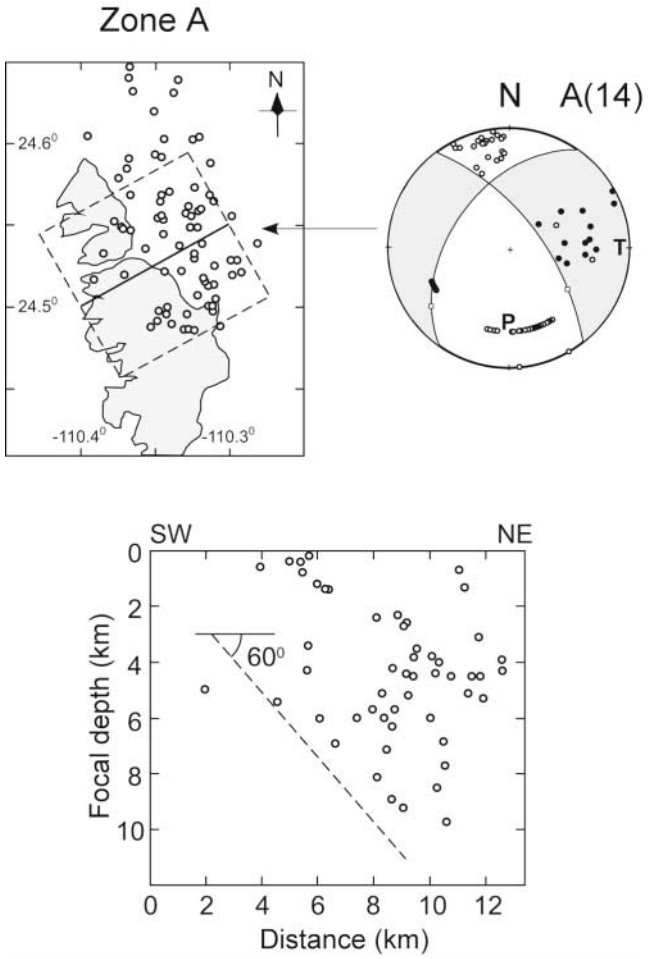

Figure 4. Map of epicenters, vertical cross section, and composite fault-plane solution for earthquakes of the Espíritu Santo and La Partida Islands area. The number of events used in the preparation of the focal mechanism is indicated in parentheses. Only earthquakes enclosed by the rectangular area on the map were included in the southwest–northeast focal depth profile.

Regarding zone H, we see that not many microearthquakes were located there. Despite this, a vertical cross section (not shown) prepared with a limited number of events barely suggests that the focal depth increases eastward. This observation, however, is not firmly supported by data. On the other hand, the fault-plane solution for this zone is consistent with the focal mechanism that Molnar (1973) reported for a M_S 5.6 earthquake located just east of Cerralvo Island (Fig. 2). This earthquake occurred on April 1969 and had its epicenter at approximately 30 km northeast of zone H. Note that these focal mechanisms are quite similar to the mechanisms of the 30 June 1995 earthquakes, with epicenters north-northwest of zone H. Moreover, these focal mechanisms, together with those of zones A, B, and G strongly suggest that along the southwestern margin of the Gulf of California normal faulting (east-side down) is the type of motion that predominates.

For the remaining areas of earthquake activity either we did not have enough information to obtain reliable focal depths (zones D and E), or the vertical depth profiles did not show any depth increase at all (zones C and G).

We emphasize here that the microearthquakes studied were not generated by the main Gulf of California fault system that forms the boundary between the Pacific and North America plates. Our overall results, then, are evidence of subsidiary faulting in a wide zone of deformation across which part of the Pacific-North America relative motion takes place. Such internal deformation of the Pacific plate, in turn, agrees with the hypothesis that capture of the Baja California peninsula by the Pacific plate has been an ongoing process through the last 3.6 Ma (DeMets, 1995; DeMets and Dixon, 1999; Dixon *et al.*, 2000; Fletcher and Munguía, 2000), with rifting and seafloor spreading in the Gulf Extensional Province overlapping during this period.

Discussion of Focal Mechanisms

In Figure 7 we show projections (onto the equatorial plane) of the *P* and *T* axes of deformation that were obtained from fault plane solutions for (1) La Paz–Los Cabos events, and (2) for 13 representative events of the Gulf of California fault system ($5.6 \leq M \leq 6.6$). The azimuth and plunge angles of Figure 7b were determined graphically from focal mechanisms published by Goff *et al.* (1987) for Gulf of California earthquakes occurring between 1963 and 1984. Even though those earthquakes occurred along faults that lie between the Delfin Basin and the Tamayo fracture zone, it is worth noting the small range of variability in the data. In addition, to give an idea about the vertical angles that the *P* and *T* axes make with the horizontal, the projected axes end at their correspondent plunge angles. A scale for plunge angle is given by means of the concentric circles included in Figure 7. With such a scale, the longer the projected lines, the more horizontal the *P* or *T* axes are.

Figure 7a provides an approximated idea of the style of deformation that prevails in the La Paz–Los Cabos region. Several specific features of interest may be observed on this figure. First, we note that most axes of minimum compressive stress are nearly horizontal. The global average of minimum compressive stresses in the region (T_{LPC}) trends in a N61° E direction with average plunge angle of about 7°. Such a result is indicative of dominant normal faulting across the region. This would be particularly true for earthquakes of zones A, B, C, G, and H, for which the mean plunge angle and trend of the *P* axis are approximately 55° and N12° W, respectively. For those zones, the average trend of the *T* axis is N68° E. The earthquake activity in such zones is produced by a series of north-northwest-striking normal faults (east-side down) that are disposed throughout the region in a domino style. As documented by Fletcher *et al.* (2000), such faults are most likely the result of westward tilting of the crystalline basement that is exposed in the Sierra la Laguna.

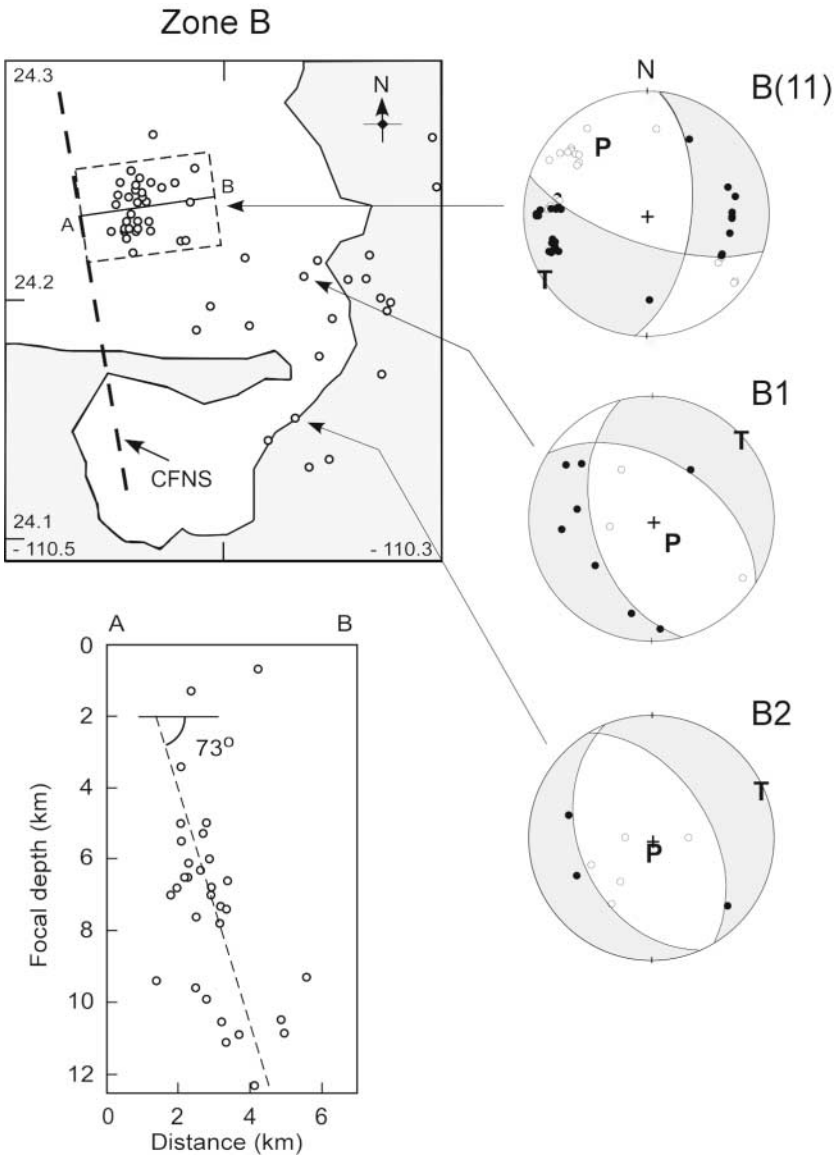

Figure 5. Map of epicenters, vertical cross section, and fault-plane solutions for earthquakes of the La Paz Bay area. The dashed line represents a possible strand of the El Carrizal fault (CFNS). The mechanisms labeled B1 and B2 are single-event fault-plane solutions for the events indicated by the arrows. Only earthquakes enclosed by the rectangular area on the map were included in the focal depth profile.

Mechanisms for zones D, E, and F, on the other side, show *T* axes that are nearly horizontal, but with mean plunge angle and direction of *P* axes that are about 20° and N38° W, respectively. Thus, A rotation of the *P* axis toward lower vertical angles seems to exist as one goes from northeast to southwest in the region. In addition, at the southwest part of the study area, the earthquakes have focal mechanisms that show predominant components of strike-slip motion, consistent with the results of Molnar (1973) (Fig. 2 and 6). These mechanisms clearly differ from the normal fault mechanisms of the northern part of the study area, but they look more like the strike-slip mechanisms for earthquakes of the Gulf of California fault system (e.g., Goff *et al.*, 1987). Our fault-plane solutions show *T* axes that are near horizontal and *P* axes that are more vertical (20°) with respect to the average plunge of the *P* axis for Gulf of California events (~9° see Fig. 7b).

Normark and Curray (1968) reported a series of subparallel north–south-trending faults, down-thrown toward the east, in the area of Cañón Las Tinajas, to the east of the 1969 Pacific events. Based on lithologic and bathymetric correlations, these researchers observed that faults in the Cañón Las Tinajas area could have also accommodated either right- or left-lateral strike-slip motion. Assuming that the 1969 Pacific earthquakes were the result of faulting in that area, Molnar (1973) chose the north-trending nodal planes of his mechanisms as the fault planes. However, as stated in Molnar's article, it is worth noticing that the nodal planes for the 1969 events are rather loosely constrained by data. Then, it may be equally plausible that the west-northwest-striking planes represent the fault on which the 1969 activity took place. In this case, activity on the fault would be characterized primarily by right-lateral strike-slip motion. This hypothesis is supported by an abundance of west-northwest-trending faults that exist in the area that extends from Todos Santos to San José Del Cabo. On the other hand, note

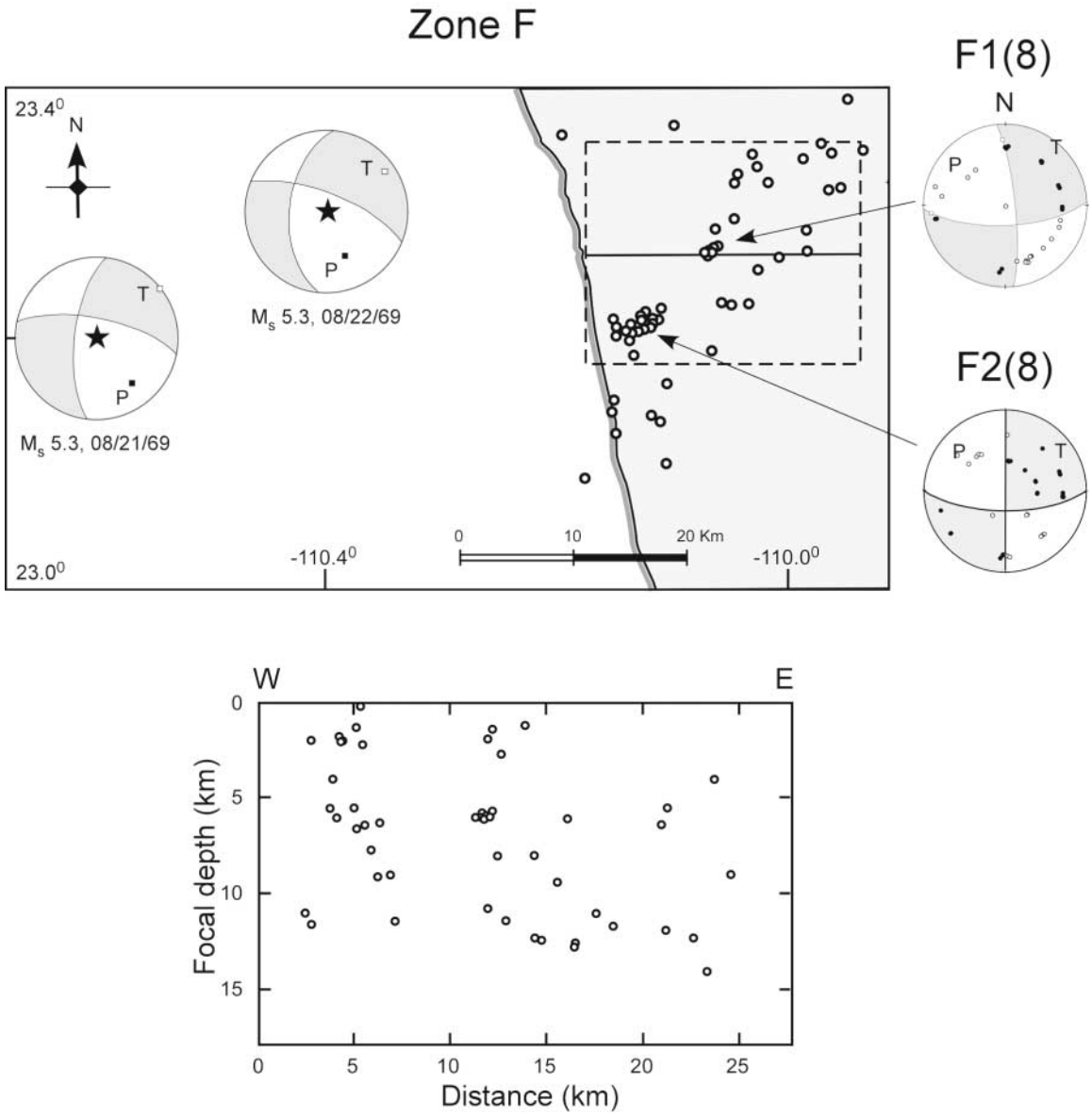

Figure 6. Map of epicenters, vertical cross section, and fault-plane solutions for earthquakes of the Pescadero-Matancitas area. For comparison purposes, the figure includes focal mechanisms for two *M* 5.3 events occurring in August 1969 (Molnar, 1973). Each focal mechanism is centered at the epicenter of the corresponding event (stars). The focal depth profile includes only the earthquakes that are enclosed by the rectangular area.

that the epicenters of such historical events were located at 30 to 50 km west of Cañón Las Tinajas. Thus, it is likely that such events could have been generated by other faults in the continental borderland of Baja California (Fletcher and Munguía, 2000). Nonetheless, earthquakes of the southwest portion of the study area have focal mechanisms with a large component of strike-slip faulting.

On the other hand, it is well established that *P* and *T* axes that are obtained from fault-plane solutions of earthquakes caused by slip on pre-existing fault surfaces are only approximations to the principal stresses (McKenzie, 1969). A fault once established becomes a plane of weakness, with later motions that might not be simply related to principal stress directions. In highly fractured zones of the Earth's crust, then, sliding on pre-existing faults is favored over the formation of fresh faults (see also Stein and Wysession, 2003). Here, we have analyzed microearthquakes that originated within the Earth's crust. Most events resulted from slippage along a set of predominant north-northwest-striking faults of the La Paz–Los Cabos region. Because of this style of faulting the axes of stress deformation on Figure 7a look relatively coherent. However, based on McKenzie (1969), it

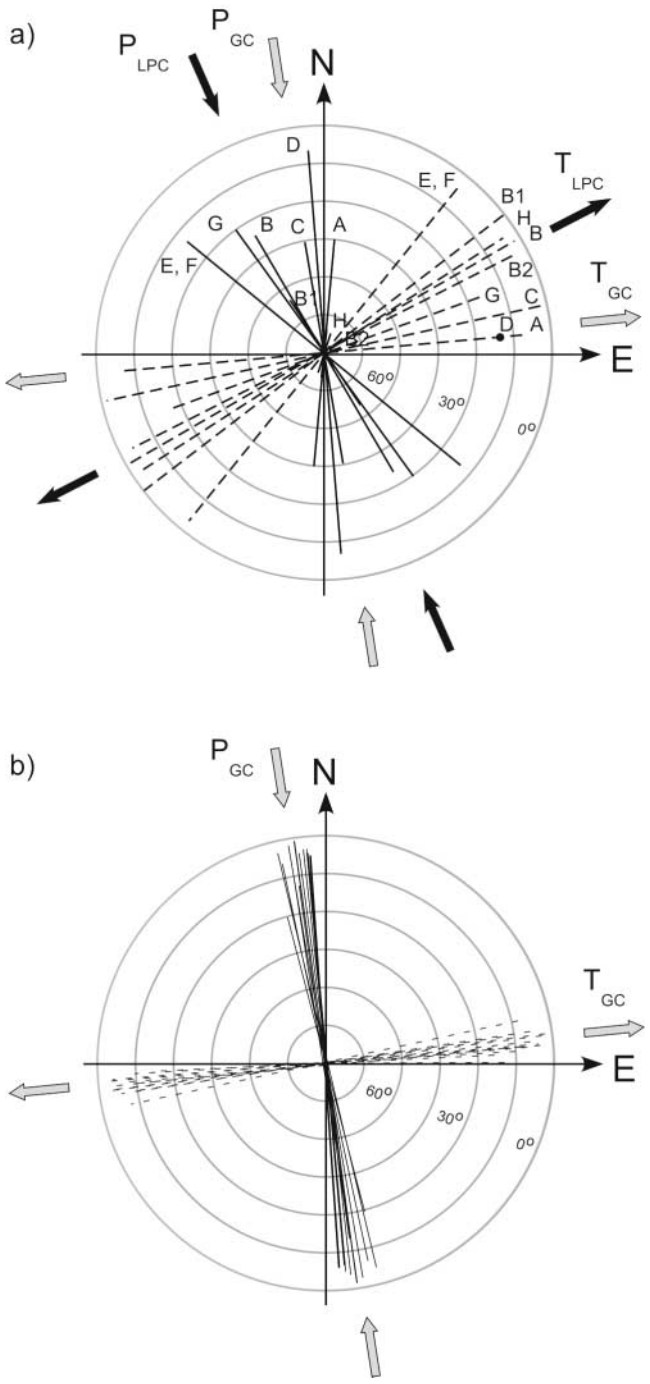

Figure 7. (a) Projections onto the equatorial plane of P (continuous lines) and T (dashed lines) axes of deformation for La Paz–Los Cabos events. The letters indicate zones of earthquakes for which focal mechanisms were calculated. (b) Similar to (a) but data correspond to 13 events of the Gulf of California ($5.6 \leq M \leq 6.6$) that occurred from 1963 to 1984 (Goff *et al.*, 1987). Each projected axis ends at its correspondent value of plunge angle, for which the concentric circles included provide a scale. Then, the longer the trend lines, the more horizontal the P or T axes they are. Black and gray arrows represent average orientations of minimum (T_{LPC}, T_{GC}) and maximum (P_{LPC}, P_{GC}) compressive stresses for the La Paz–Los Cabos and Gulf of California regions, respectively.

might happen that our determined P and T axes only partially reflect the regional stress field. As shown in Figure 7, the global average compressive stresses for the La Paz–Los Cabos (P_{LPC} and T_{LPC}) and the Gulf of California (P_{GC} and T_{GC}) regions were found to be different. This is particularly true for the northern part of the study area, in which the P-stress axes have more vertical plunge angles (55°) in comparison with the subhorizontal plunge angles of the Gulf events (9°). In addition, the orientation of the tension axis T_{LPC} is 16–22° more northeasterly than T_{GC}. These differences in stress-axis orientations suggest either that earthquakes in the study region occur more in response to local tectonic forces than to the regional stress field, or that our determined mean P and T axes are only approximations of the regional principal stresses. Although the complex tectonic situation of the study area makes the first possibility feasible, the fact that most analyzed events occurred on preexisting faults of the region is in favor of the second one. Then, because of the rather scarce focal mechanism data analyzed here, these preliminary results, in particular, must be viewed with caution. After this attempt, more seismic data are needed to achieve better results in relation to the regional stress pattern.

Conclusions

We analyzed seismic data recorded for seven years in the La Paz–Los Cabos region. Our dataset included events with moment magnitudes of up to 3.6 and focal depths that are mostly between 2 and 14 km. At the initial stage of the study, an intense activity was observed along the east flank of the Espíritu Santo and La Partida islands. This activity, which ceased by December 1999, was considered to be part of the aftershock series that followed the 30 June 1995 La Paz earthquakes. Many other microearthquakes occurred scattered all over the study area. Some of them correlated with known faults of the region, but others did not, suggesting faults that have not been recognized geologically. In addition, zones of stress concentration were identified in the region. In such zones the seismicity often developed as swarms of earthquakes.

Focal mechanisms determined for events of the northern part of the study area indicated normal faulting (east-side down). In such case, the P axis had a mean vertical angle of 55° in the N12° W direction, whereas the T axis was nearly horizontal, with a N68° E average trend. It was concluded that this part of the study area is under a predominant tensional stress regime. At the southwest part of the study area, the focal mechanisms showed predominant components of strike-slip faulting. There, the T axes were still subhorizontal, but the P axes showed lower vertical angles, resulting in a mean plunge of about 20° in the N38° W direction.

Average directions of P and T axes were obtained from data of 13 representative earthquakes of the Gulf of California fault system. The highly consistent results obtained led to average stress directions that seem near representa-

tions of the principal stresses that drive this fault system. A comparison of these axes with the average *P*- and *T*-stress axes of our region shows that the latter are approximately 16–23° more westerly than the former. On this basis, we propose either that earthquakes in the study area occur more in response to local tectonic forces or that our inferred *P* and *T* axes are only approximations to the regional principal stresses. Although the complex tectonic situation of the study area makes the first possibility feasible, the fact that most analyzed events occurred on pre-existing faults of the region could be in favor of the second one. These particular results must be viewed cautiously because of the rather scarce focal mechanism data used.

Finally, the micro earthquakes studied here were not generated by the main Gulf of California fault system that forms the main boundary between the Pacific and North America plates. Our results are thus evidence of a wide zone of deformation across which subsidiary faulting accommodates part of the relative plates motion.

Acknowledgments

We thank Miguel Navarro Sánchez and Tito A. Valdéz López for their support in the installation and operation of the seismic stations. We also thank Antonio Vidal Villegas and two anonymous reviewers for helpful comments on the manuscript. Financial support for this study was provided by the Consejo Nacional de Ciencia y Tecnología (CONACYT, Contract GT-26750) and Centro de Investigación Científica y de Educación Superior de Ensenada, B.C. (CICESE).

References

Aranda-Gómez, J. J., and J. A. Pérez-Venzor (1997). Active faults in the Los Cabos block, Baja California Sur, México, Compilation for the map of major active faults, western hemisphere, International Lithosphere Program (ILP), Project II-2, 27 pp.

Atwater, T. (1970). Implications of plate tectonics for the Cenozoic tectonic evolution of western North America, *Geol. Soc. Am. Bull.* **81,** 3513–3536.

Atwater, T. (1989). Plate tectonic history of the northeast Pacific and western North America, in *The Eastern Pacific Ocean and Hawaii*, E. L. Winterer, D. M. Hussong, and R. W. Decker (Editors), Geological Society of America, Boulder, Colorado, 21–72.

Bohannon, R. G., and T. Parsons (1995). Tectonic implications of post-30 Ma Pacific and North American relative plate motions, *Geol. Soc. Am. Bull.* **107,** 937–959.

Bravo-Pérez, J. R. (2002). Segmentación de la falla San José del Cabo y su relación con la evolución tectonoestratigráfica de la Cuenca San José del Cabo, Baja California Sur, México, *Masters thesis*, Centro de Investigación Cientifica y de Educación Superior de Ensenada, B. C., Ensenada, Baja California, México, 226 pp.

DeMets, C. A. (1995). Reappraisal of seafloor spreading lineations in the Gulf of California: implications for the transfer of Baja California to the Pacific plate and estimates of Pacific-North America motion, *Geophys. Res. Lett.* **22,** 3545–3548.

DeMets, C. A., and T. H. Dixon (1999). New kinematic models for Pacific-North America motion from 3 Ma to present, I: evidence for steady motion and biases in the NUVEL-1A model, *Geophys. Res. Lett.* **26,** no. 13, 1921–1924.

Dixon, T., F. Farina, Ch. De Mets, F. Suárez-Vidal, J. Fletcher, B. Márquez-Azua, M. Miller, O. Sánchez, and P. Umhoefer (2000). New kinematic models for Pacific-North America motion from 3 Ma to present, II: evidence for a "Baja California shear zone," *Geophys. Res. Lett.* **27,** no. 23, 3961–3964.

Fletcher, J. M., and L. Munguía (2000). Active continental rifting in southern Baja California, México: implications for plate motion partitioning and the transition to seafloor spreading in the Gulf of California, *Tectonics*, **19,** no. 6, 1107–1123.

Fletcher, J. M., B. P. Kohn, D. A. Foster, and A. J. W. Gleadow (2000). Heterogeneous neogene cooling and exhumation of the Los Cabos block, southern Baja California: evidence from fission-track thermochronology, *Geology* **28,** no. 2, 107–110.

Goff, J. A., E. A. Bergman, and S. C. Solomon (1987). Earthquake source mechanisms and transform fault tectonics in the Gulf of California, *J. Geophys. Res.* **92,** 10,485–10,510.

Havskov, J., and L. Ottemöller (Editors) (2001). SEISAN: the earthquake analysis software for Windows, SOLARIS, and LINUX, Version 7.2. Manual, Institute of Solid Earth Physics, University of Bergen, Norway.

Humphreys, E. D., and R. J. Weldon, II (1991). Kinematic constraints on the rifting of Baja California, in *The Gulf and Peninsular Province of the Californias*, J. P. Dauphin and B. R. T. Simoneit (Editors), American Association of Petroleum Geologists Memoir 47, 217–229.

Kanamori, H. (1977). The energy release in great earthquakes, *J. Geophys. Res.* **82,** 1981–1987.

Kanamori, H., and P. C. Jennings (1978). Determination of local magnitude, M_L, from strong motion accelerograms, *Bull. Seism. Soc. Am.* **68,** 471–485.

Lee, W. H. K., R. E. Bennet, and K. L. Meagher (1972). A method of estimating magnitude of local earthquakes from signal duration, *U.S. Geol. Surv. Open-File Rept.*, 28 pp.

Lienert, B. R. E., and J. Havskov (1995). A computer program for locating earthquakes both locally and globally, *Seism. Res. Lett.* **66,** 26–36.

McKenzie, D. P. (1969). The relation between fault plane solutions for earthquakes and the directions of the principal stresses, *Bull. Seism. Soc. Am.* **59,** no. 2, 591–601.

Minster, J. B., and T. H. Jordan (1987). Vector constraints on western U.S. deformation from space geodesy, neotectonics and plate tectonics, *J. Geophys. Res.* **92,** 4798–4804.

Molnar, P. (1973). Fault plane solutions of earthquakes and direction of motion in the Gulf of California and in the Rivera fracture zone, *Geol. Soc. Am. Bull.* **84,** 1651–1658.

Munguía, L., J. Gaitán, V. Wong, and S. Mayer (1992). Microsismicidad en la zona de la falla La Paz, Baja California Sur, México, *Geofís. Int.* **31,** no. 3, 279–287.

Normark, W. R., and J. R. Curray (1968). Geology and structure of the tip of Baja California, México, *Geol. Soc. Am. Bull.* **79,** 1589–1600.

Normark, W. R., J. E. Spencer, and J. C. J. Ingle (1987). Geology and Neogene history of the Pacific Continental Margin of Baja California Sur, Mexico, in *Geology and Resource Potential of the Continental Margin of Western North America and Adjacent Basins—Beaufort Sea to Baja California*, D. W. Scholl, A. Grantz, and J. G. Vedder (Editors), Circum-Pacific Council for Energy and Mineral Resources, Houston, Texas, 449–472.

Ottemöller, L., and J. Havskov (2003). Moment magnitude determination for local and regional earthquakes based on source spectra, *Bull. Seism. Soc. Am.* **93,** no. 1, 203–214.

Richter, C. F. (1958). *Elementary Seismology*, W. H. Freeman, San Francisco, 768 pp.

Snoke, J. A., J. W. Munsey, A. G. Teague, and G. A. Bollinger (1984). A program for focal mechanism determination by combined use of polarity and SV-P amplitude ratio data, *Earthquake Notes* **55,** 15.

Stein, S., and M. Wysession (2003). *An Introduction to Seismology, Earthquakes, and Earth Structure.* Blackwell, Oxford.

Weldon, R., and E. Humphreys (1986). A kinematic model of southern California, *Tectonics* **5,** 33–48.

División de Ciencias de la Tierra
Centro de Investigación Científica y de Educación Superior
de Ensenada, B.C.
Km 107 Carretera Tijuana-Ensenada, Ensenada
Baja California, C. P. 22860, México
lmunguia@cicese.mx
(L.M., M.G.)

Centro de Investigación Científica y de Educación Superior
de Ensenada, B.C.
Unidad La Paz, Baja California Sur
Miraflores 334, Fracc. Bellavista
La Paz, Baja California Sur, C. P. 23050, México
(S.M., A.A.)

Manuscript received 1 June 2005.